

Early Detection of Aggregation in Formulations

FlowCam Nano for submicron particle characterization in biotherapeutics

SUMMARY

Effective particle monitoring strategies are essential in the development and production of safe biotherapeutics as these particulates can drastically impact patient therapy outcomes. Flow Imaging Microscopy (FIM) is an increasingly prominent technique for determining the number, size, and types of subvisible particles 2 - 100 μm in diameter in biotherapeutic samples.

FlowCam Nano extends this analysis to small subvisible and submicron particles (particles 300 nm - 2 μm in diameter), which are too small for traditional FIM instruments to image effectively. Submicron FIM allows users to detect particle sources like API aggregation and bacterial contamination that initially produce particulates too small to detect by traditional imaging techniques but can agglomerate into larger subvisible particles if not addressed.

In this study, we demonstrate the utility of FlowCam Nano in biotherapeutic development by analyzing solutions containing protein aggregates, sucrose aggregates, and *E. coli* cells using traditional subvisible and submicron FIM. For each sample type, FlowCam Nano revealed particle size and shape information that would have been difficult, if not impossible, to detect with standard FIM approaches.

In a concurrent study, two FlowCam Nano instruments were also used to demonstrate their ability to accurately detect relative particle concentrations of bacteria. These studies demonstrate how FlowCam Nano may be used to detect particle sources of aggregation and bacterial contamination reliably and potentially earlier than traditional FIM.

INTRODUCTION

All biotherapeutics contain particles. Particles can originate from a variety of sources, such as the active pharmaceutical ingredient (API) and its aggregates¹⁻³, container-closure systems (e.g., silicone oil droplets^{4,5}, glass flakes⁶), contaminants from upstream processing steps, and other sources. While these particulates can be the active ingredient of a therapeutic (e.g., cells in cell-based medicinal products^{7,8}, drug delivery vehicles), they are often impurities that can potentially drastically worsen the efficacy of the therapeutic^{9,10}.

Researchers are advised to characterize particles in their biotherapeutics not just to meet regulations such as USP <788>, but to identify and control sources of particle formation and maximize the safety and efficacy of their therapeutic. New, more sensitive techniques are therefore critical to ensure the safety of these therapies.

Flow imaging microscopy (FIM) is an increasingly popular technique for analyzing particulates in biotherapeutics¹¹⁻¹³. FIM instruments like FlowCam use a combination of microfluidics and light microscopy to automatically capture images quickly and in large quantities. These images can be used to analyze the concentration, size distribution, and morphology of particles in a biotherapeutic sample. Users can then analyze this information alongside that from orthogonal techniques to make a useful overall assessment of sample quality.

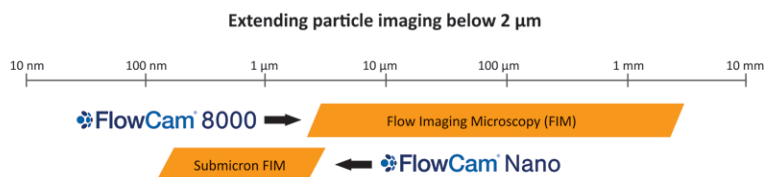


Figure 1. Size ranges of FlowCam Nano and FlowCam 8000 series instruments

Typical FIM instruments are designed to analyze subvisible particles larger than 2 μm in diameter (see Figure 1 and Table 1). While these subvisible particles have received significant attention from researchers^{2,10}, there is increasing interest in analyzing smaller submicron particles (i.e. particles between 100 nm and 1 μm) in biopharmaceuticals outside the size range of traditional imaging techniques. While these objects are not directly subject to regulations like USP <787/788>, particles in this size range can agglomerate or otherwise promote the formation of larger subvisible particles^{3,14} that are subject to these regulations. A technique like FIM for analyzing these submicron particles would allow the user to detect sources of particle generation such as protein and sucrose aggregation early before additional agglomeration occurs. Additionally, some objects exhibit a narrow size distribution near or below the size range of typical FIM instruments (e.g., bacterial cells, some drug delivery vehicles) and require a submicron-focused approach to be detected.

Name	Size Range
Nanoparticles	10-100 nm
Submicron Particles	0.1-1 μm
Subvisible Particles	1-100 μm
Visible Particles	>100 μm

Table 1. Common definitions for different particle sizes. FlowCam 8100 and other FIM instruments focus on subvisible particles, FlowCam Nano focuses on submicron particles.

FlowCam Nano was recently introduced as a novel particle analysis technique for detecting and analyzing submicron particles. The instrument employs a patented modification of FIM that uses an oil immersion-based light microscopy system to capture images with 40X magnification (Figure 2). This allows the instrument to detect particles between 300 nm and 2 μm - the smallest objects visible with light microscopy. Particulates in this size range are not only missed by traditional flow imaging microscopy, but are often challenging to characterize with other particle analysis instruments, many of which are either ensemble techniques or do not provide morphology information. Like traditional FIM instruments, FlowCam Nano records size and morphology information for each particle—information that can be useful in identifying the types of submicron particulates in a sample.

The shallow depth of field used by the instrument is designed to maximize image quality and thus the morphology information available from the instrument. While this depth of field results in some objects being out of focus and thus not detected, the relative particle counts reported by the instrument are consistent between samples, allowing FlowCam Nano to also be used for monitoring the relative particulate levels. The unit can also be operated in a calibrated count mode which provides accurate particle counts for samples containing dark, easily detectable objects similar to polystyrene latex calibration beads. FlowCam Nano also retains the high-throughput and ease-of-use benefits of typical FIM instruments, allowing for fast and efficient particle imaging, especially relative to manual oil-immersion microscopy.

To demonstrate the utility of FlowCam Nano in biotherapeutic development, this study compares the size distribution and images of subvisible particles detected by FlowCam 8100 to submicron particles detected by FlowCam Nano. Three potential impurities in therapeutic protein formulations were analyzed on both instrument types: protein aggregates, sucrose aggregates, and contaminating bacteria. We also used FlowCam Nano to measure the concentrations of a bacteria culture at various dilutions to assess the counting performance of the instrument.

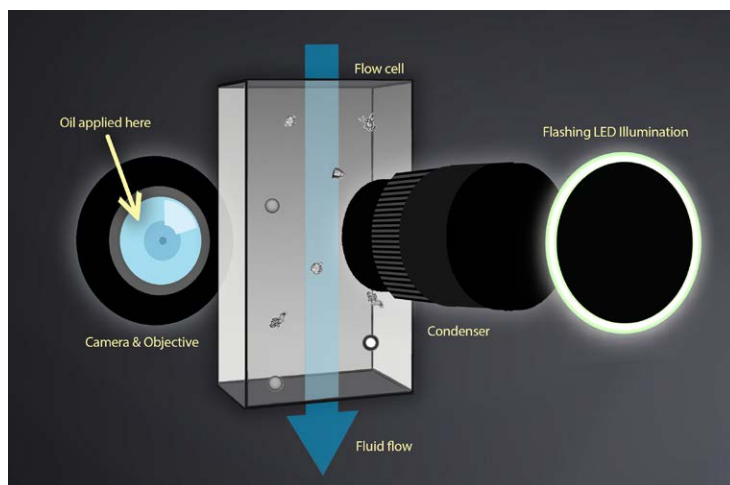


Figure 2. Schematic of immersion oil-based flow imaging microscopy, the technology that FlowCam Nano uses to image submicron particles

MEASUREMENTS & METHODS

Materials: Bovine serum albumin (BSA) powder, sucrose, and phosphate buffered saline (PBS) were obtained from Sigma-Aldrich (St. Louis, MO). *E. coli* cultures were obtained from Carolina Biological Supply (Burlington, NC). 700 nm and 15 μm Duke Standards polystyrene microspheres were used to focus the FlowCam Nano and FlowCam 8100, respectively. Immersion oil for the FlowCam Nano was obtained from ibidi (Fichburg, WI). Micro-90 was obtained from International Products Corp. (Burlington, NJ).

Sample preparation: Samples containing protein aggregates, sucrose particles, and *E. coli* cells in PBS were prepared for FIM analysis. 15 mL of 1 mg/mL BSA solution in PBS was prepared and vortexed to generate protein aggregates. To generate sucrose particles, 25 mL of PBS containing 5% w/v sucrose was heated to 37° C for two hours with constant mixing and then incubated overnight at room temperature.

E. coli cultures were serially diluted in PBS to obtain samples containing different concentrations of bacterial cells. The *E. coli* culture as received from Carolina Biological was diluted 1:100 with PBS to generate a sample containing an appropriate concentration for FIM analysis. This “stock” solution was then diluted to 1:2, 1:4, 1:8, and 1:16 to get samples containing different concentrations of bacteria.

Flow Imaging Microscopy (FIM): FlowCam 8100 and FlowCam Nano instruments (Yokogawa Fluid Imaging Technologies; Scarborough, ME) were used to analyze the particulate contents of the samples described in the previous section. Instrument operation and data analysis was performed using VisualSpreadsheet® 5.8 for all experiments on both FlowCam models. Both instruments were

focused on polystyrene latex calibration beads using the built-in autofocus software for each instrument. The FlowCam 8100 unit was focused using 15 μm beads while the FlowCam Nano units were focused using 700 nm beads. The fluidics in each instrument were cleaned with a 1% Micro-90 solution followed by PBS before measurements and with PBS between samples.

FlowCam 8100 was equipped with a 10X objective, an FOV80 flow cell, and a grayscale camera. 1 mL aliquots of sample were analyzed at a 150 $\mu\text{L}/\text{min}$ flow rate. Particle detection was performed using 15 dark and 15 light pixel thresholds, four close hole iterations, and 4 μm distance to nearest neighbor for the segmentation. Imaged objects 2-10 μm in diameter were used in this analysis.

FlowCam Nano was equipped with the default 40X objective, a 60 μm flow cell, and grayscale camera. 250 μL aliquots of sample were analyzed at a 25 $\mu\text{L}/\text{min}$ flow rate. Each sample was analyzed using relative count mode. The protein aggregate and sucrose particle samples were analyzed using 20 dark and 18 light pixel thresholds, 3 close hole iterations, and 0.1 μm distance to nearest neighbor. To account for their more transparent particles, *E. coli* samples were analyzed using a 12 light pixel threshold, 4 close hole iterations, and 1 μm distance to nearest neighbor for the segmentation. An edge gradient filter of 25 was also used for each sample type to remove out-of-focus or otherwise blurry images. All other detected objects in the size range of the instrument were used in this analysis.

The protein aggregate, sucrose particle, and stock *E. coli* samples were analyzed using both FlowCam Nano and FlowCam 8100 to compare the particles detected and the size distribution reported by the two instruments. Three aliquots of each sample were imaged on each instrument. All images collected from each sample type when analyzed on a single FlowCam model were pooled together and used to estimate the particle size distribution and select images for that sample.

Samples containing dilutions of the stock *E. coli* solution were analyzed on FlowCam Nano to assess if the reported particle concentrations were linear with the fraction of stock solution in the sample. To evaluate instrument and operator variability, *E. coli* samples at the dilutions listed in the previous section were analyzed on two FlowCam Nano instruments by two different analysts. Both units were set up as described above. For each unit and bacterial cell concentration, a single 400 μL aliquot of sample was loaded on the instrument and 300 μL of that sample was analyzed. The resulting dilution-particle concentration data was then analyzed for each instrument separately via linear regression to check for linearity.

RESULTS & DISCUSSION

FlowCam Nano and FlowCam 8100 Comparison

Protein aggregates, sucrose particles, and *E. coli* cells were analyzed on both a traditional FIM instrument (FlowCam 8100) and a FlowCam Nano instrument. Figure 3 shows the average particle size distributions obtained for each sample on both FlowCam 8100 and FlowCam Nano. FlowCam 8100 returned similar particle size distributions for each sample (Figure 3, right column); the concentration of particles in a specific size range increased with decreasing size with those 2-3 μm in size making up the bulk of the objects detected in each sample. This asymmetric size distribution suggests that each sample contained many additional particulates smaller than 2 μm that were not detected by FlowCam 8100 - a suggestion confirmed by the FlowCam Nano measurements.

The size distributions measured by FlowCam Nano (Figure 3, left) varied between the three samples. For the protein aggregate (Figure 3, top row) and sucrose (Figure 3, middle row) samples, the size distribution returned by FlowCam Nano exhibited the same trend as FlowCam 8100: the samples contained higher concentrations of smaller particles than larger ones.

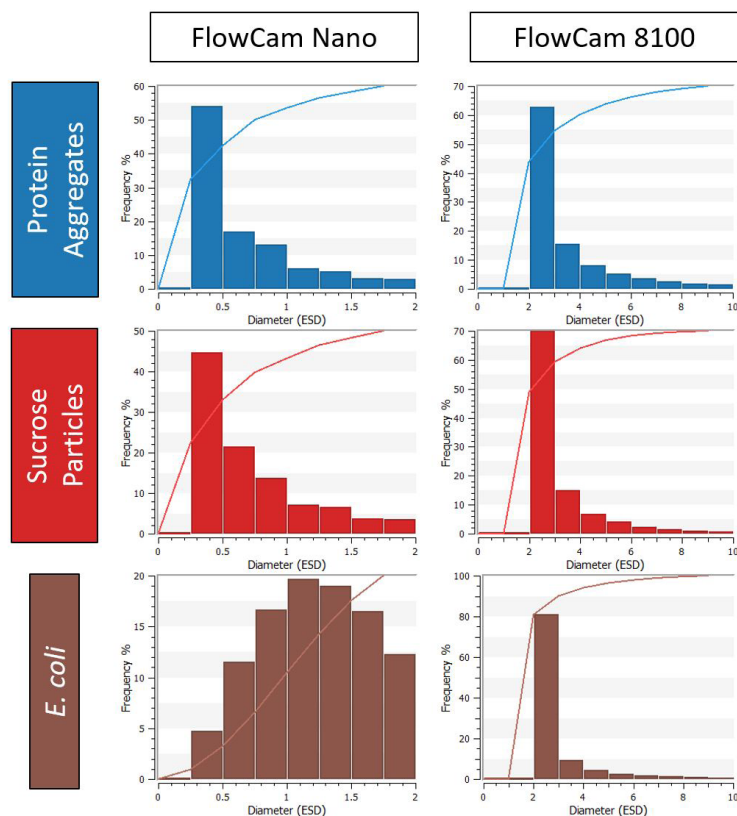


Figure 3. Particle size distributions for samples containing protein aggregates (top row), sucrose particles (middle row), and *E. coli* cells (bottom row). Size distributions were obtained using FlowCam Nano (left) and FlowCam 8100 (right). Bars indicate the fraction of particles captured by each instrument in the corresponding size bin. The corresponding line graph indicates the fraction of particles captured by each instrument smaller than the corresponding size.

For these samples, FlowCam Nano detected a relatively larger fraction of the overall particle content of the sample than the typical FIM instrument. As suggested by this behavior, FlowCam Nano may be able to detect protein aggregation and other degradation pathways early and before they generate subvisible particles detectable via FlowCam 8100.

Unlike the other samples, *E. coli* (Figure 3, bottom row) exhibited a size distribution with a peak between 1 and 1.25 μm —roughly the size of a single *E. coli* cell. As further confirmation of the particle identity, the aspect ratio distribution for these cells (Figure 4) shows a peak between 0.2 and 0.3, agreeing with the nominal 0.25 aspect ratio of the organism (0.5 μm thick, 2 μm long). The size distribution suggests that FlowCam Nano detected not only a larger proportion of the *E. coli* cells than the 8100 but a majority of the total *E. coli* cells in this sample. Due to the narrow size distribution of these cells and the limited fraction of these cells above the lower size limit of FlowCam 8100, FlowCam Nano is better suited for detecting bacterial contamination of biotherapeutic samples and manufacturing equipment than FlowCam 8100 and other standard imaging methods.

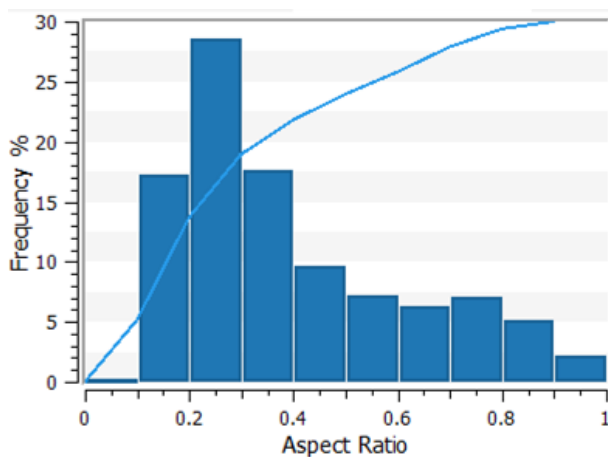


Figure 4. Particle aspect ratio for *E. coli* cells measured via FlowCam Nano. The format of this plot matches that of the size distributions in Figure 2.

Sample images of all three particle types from both instruments are shown in Figure 5. Small particles resulted in low-detail images by FlowCam 8100, which makes it challenging to distinguish different morphologies. In contrast, FlowCam Nano returned much more detailed images of these small objects. These images allow users to easily distinguish images of *E. coli* from those of other particle types and may also help users distinguish between images of protein aggregates and sucrose particles. While a bacteria-contaminated biological sample would be difficult to detect using typical FIM images, it would be simple to identify this type of contamination using FlowCam Nano due to the stark contrast between images of bacteria and those of more common biotherapeutic particulates.

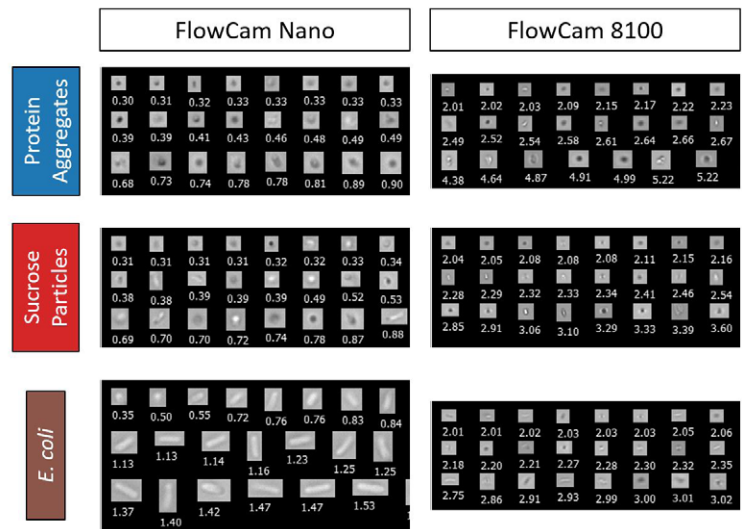


Figure 5. FlowCam Nano (left column) and FlowCam 8100 (right column) images of protein aggregates (top row), sucrose particles (middle row), and *E. coli* cells (bottom row). Images are approximately to-scale with other images from that instrument. Equivalent spherical diameter values (in μm) for each particle are shown below their image.

FlowCam Nano Particle Concentration Consistency

Additional experiments were performed on diluted *E. coli* samples on two FlowCam Nano instruments to assess the relative accuracy of the reported particle concentrations. Figure 6 shows the particle concentrations reported by the two units at different dilutions of the *E. coli* solution analyzed above. While there is some disagreement between the absolute concentrations reported by both instruments, both instruments exhibited great linearity between the amount of sample dilution and the observed particle concentration as indicated by the high R^2 values obtained from linear regression. These results demonstrate that FlowCam Nano yields self-consistent particle concentrations that can be used to monitor the relative amounts of submicron particles in a sample as well as their size and shape.

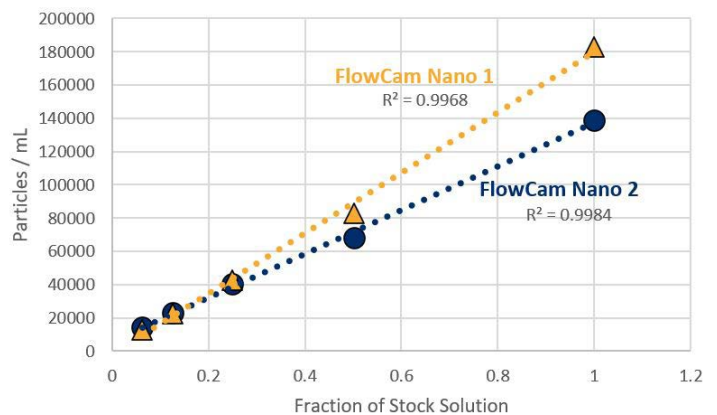


Figure 6. Particle concentrations measured at different dilutions of an *E. coli* sample. Circles and triangles each represent measurements from a single FlowCam Nano. Lines represent linear fits for the corresponding instrument's concentration data. R^2 values for each trendline are shown next to each line.

CONCLUSIONS

FlowCam Nano is a promising submicron particle analysis tool, capturing particle size and type information that extends the typical size range of traditional FIM. Additionally, FlowCam Nano provides particle concentrations that are consistent with the particle content of the sample. This information is invaluable in analyzing properties of particles like sucrose, bacterial cells, and certain drug delivery vehicles that are typically below the size range imaged by traditional FIM. Information on these smaller objects can also be valuable even for identifying particle types commonly encountered in the subvisible range like protein aggregates that often form in part from the agglomeration of smaller particles. Analyzing these smaller submicron protein aggregates can help the user identify these objects before they can agglomerate and form larger particles.

The submicron particle characterization provided by FlowCam Nano complements other analysis techniques. FlowCam Nano provides the user access to particle morphology information that is not available from other modalities - information that can be used to determine the types of submicron particles in a sample (e.g., bacteria cells and more common biopharmaceutical particles and contaminants). FlowCam Nano can also be used to extend the particle count and size distribution available from FlowCam 8100 and other typical FIM instruments, resulting in an overall larger size range than either instrument provides on its own. This combined information can help the user get a better understanding of the particle content in their biopharmaceutical samples and thus make faster, more-informed decisions about product quality.



**FlowCam Nano flow imaging microscope
by Yokogawa Fluid Imaging Technologies**



Distributed by:
Kenelec Scientific Pty Ltd
1300 73 22 33
sales@kenelec.com.au
www.kenelec.com.au



REFERENCES

1. Chi EY, Krishnan S, Randolph TW, Carpenter JF. Physical stability of proteins in aqueous solution: Mechanism and driving forces in nonnative protein aggregation. *Pharm Res.* 2003;20(9):1325-1336. doi:10.1023/A:1025771421906
2. Carpenter JF, Randolph TW, Jiskoot W, et al. Overlooking Subvisible Particles in Therapeutic Protein Products: Gaps That May Compromise Product Quality. *J Pharm Sci.* 2009;98:1201-1205.
3. Roberts CJ. Therapeutic protein aggregation: Mechanisms, design, and control. *Trends Biotechnol.* 2014;32(7):372-380.
4. Gerhardt A, McGraw NR, Schwartz DK, Bee JS, Carpenter JF, Randolph TW. Protein aggregation and particle formation in prefilled glass syringes. *J Pharm Sci.* 2014;103(6):1601-1612.
5. Krayukhina E, Tsumoto K, Uchiyama S, Fukui K. Effects of syringe material and silicone oil lubrication on the stability of pharmaceutical proteins. *J Pharm Sci.* 2015;104(2):527-535.
6. Ennis RD, Pritchard R, Nakamura C, et al. Glass vials for small volume parenterals: Influence of drug and manufacturing processes on glass delamination. *Pharm Dev Technol.* 2001;6(3):393-405.
7. Sediq AS, Klem R, Nejadnik MR, Meij P, Jiskoot W. Label-Free, Flow-Imaging Methods for Determination of Cell Concentration and Viability. *Pharm Res.* 2018;35(8).
8. Grabarek AD, Jiskoot W, Hawe A, Pike-Overzet K, Menzen T. Forced degradation of cell-based medicinal products guided by flow imaging microscopy: Explorative studies with Jurkat cells. *Eur J Pharm Biopharm.* 2021;167(June):38-47.
9. Rosenberg AS. Effects of protein aggregates: An immunologic perspective. *AAPS J.* 2006;8(3):E501-E507.
10. Kotarek J, Stuart C, De Paoli SH, et al. Subvisible Particle Content, Formulation, and Dose of an Erythropoietin Peptide Mimetic Product Are Associated with Severe Adverse Postmarketing Events. *J Pharm Sci.* 2016;105(3):1023-1027.
11. Sharma DK, Oma P, Pollo MJ, Sukumar M. Quantification and Characterization of Subvisible Proteinaceous Particles in Opalescent mAb Formulations Using Micro-Flow Imaging. *J Pharm Sci.* 2010;99:2628-2642.
12. Zölls S, Weinbuch D, Wiggenhorn M, et al. Flow Imaging Microscopy for Protein Particle Analysis-A Comparative Evaluation of Four Different Analytical Instruments. *AAPS J.* 2013;15(4):1200-1211.
13. Narhi LO, Corvari V, Ripple DC, et al. Subvisible (2-100 μm) particle analysis during biotherapeutic drug product development: Part 1, considerations and strategy. *J Pharm Sci.* 2015;104(6):1899-1908.
14. Pardeshi NN, Zhou C, Randolph TW, Carpenter JF. Protein Nanoparticles Promote Microparticle Formation in Intravenous Immunoglobulin Solutions During Freeze-Thawing and Agitation Stresses. *J Pharm Sci.* 2018;107(7):1852-1857.